

Non-Gaussian displacements in active transport on a carpet of motile cells

Robert Großmann,^{1,*} Lara S. Bort,¹ Ted Moldenhawer,¹ Setareh Sharifi Panah,¹ Ralf Metzler,^{1,2} and Carsten Beta¹

¹*Institute of Physics and Astronomy, University of Potsdam, Potsdam 14476, Germany*

²*Asia Pacific Center for Theoretical Physics, Pohang 37673, Republic of Korea*

(Dated: November 10, 2023)

We study the dynamics of micron-sized particles on a layer of motile cells. This cell carpet acts as an active bath that propels passive tracer particles via direct mechanical contact. The resulting nonequilibrium transport shows a crossover from superdiffusive to normal-diffusive dynamics. The particle displacement distribution is distinctly non-Gaussian even in the limit of long measurement times—different from typically reported Fickian yet non-Gaussian transport, for which Gaussianity is restored beyond some system-specific correlation time. We obtain the distribution of diffusion coefficients from the experimental data and introduce a model for the displacement distribution that matches the experimentally observed non-Gaussian statistics and argue why similar transport properties are expected for many composite active matter systems.

The collective behavior of active particles is the focus of one of the most dynamically evolving research directions in nonequilibrium statistical and biological physics over the past decade. Active particles [1, 2] convert chemical energy into motion and provide a unifying concept for a wide range of systems, such as engineered bipolar ‘Janus particles’ with different sources of activity [3–6], bacterial swimming [7, 8] and swarming [9], crawling cells [10], bristle robots (hexbugs) [11–13], or groups of foraging animals [14]. Large ensembles of interacting active particles, in which energy is continuously injected and dissipated locally, operate far from thermodynamic equilibrium. This gives rise to a plethora of nonequilibrium phenomena, such as the emergence of large scale patterns [15], topological order [16], or nonequilibrium phase separations [17–19], and raises questions about the thermodynamics of such systems, e.g., their pressure [20–22]. All these features are being studied under the common theme of active matter physics [23, 24].

In many real-world settings, active agents interact with passive objects in their surroundings that introduce additional degrees of complexity (‘composite active matter’ [25]). For instance, boundaries and obstacles may rectify their motion [26], self-similar structures may emerge at interfaces in active matter invasion [27], or non-isotropic passive objects, such as gears [28, 29] or curved tracers [30] can be powered by an ‘active bath’ of self-propelled particles to perform coherent motion. For a fundamental understanding as well as for many applications, the statistics of transport in a bath of active elements is of particular importance. Earlier work has focused on tracer diffusion in active fluids composed of suspensions of biological swimmers, such as bacteria or algae, agitating the surrounding fluid of the bath [31–33], or particles in the vicinity of flow-generating active carpets [34]. Non-trivial scalings with several crossovers in the mean-squared displacement (MSD) of passive tracer particles were observed; for a review, see Ref. [2]. However, little is known about the statistical properties of

other types of active baths. A particularly large and important class are composite systems, in which the interactions between active elements and passive tracers are established by direct mechanical contact and adhesion instead of fluid flows and hydrodynamic interactions. This situation arises, for example, when slowly moving, adherent cells interact with passive objects, and it has important practical implications for the movement of foreign bodies in tissues or the delivery of drug-loaded particles in a multicellular environment.

Here we consider such a composite biohybrid system as a paradigmatic showcase of an active bath, in which passive objects are agitated and transported by self-propelled agents via direct mechanical contact. As an active bath, we use a monolayer of cells of the social amoeboid *Dictyostelium discoideum*, an established model organism with well-characterized properties [36]. As *D. discoideum* cells show unspecific adhesion to most common material surfaces [37], adhesive contacts between cells and microparticles are formed upon collision and may spontaneously break again [38]. No specific surface functionalization is required. Unbound cells can freely move over the two-dimensional substrate. When cells bind to the microparticles, the active motion of cells results in nonthermal fluctuating forces that randomly displace the particles. While this process has been studied in detail for single cells interacting with a single particle [25, 39], we here consider particles that are attached to many cells at the same time. We performed time-lapse recordings with a time interval of 15s between frames over a duration of 4 hours. In total, 174 particle trajectories were extracted; the majority were longer than 2.5 hours [35]. An example from the recorded image stacks is shown in Fig. 1(a), with the particle trajectories displayed as colored overlays (see Material and Methods in SM [35] for experimental details). From the trajectories, we characterized the dynamics of particles on the cell layer in terms of their MSD, their displacement probability density functions (PDFs), and their displacement auto-correlation function (DACF).

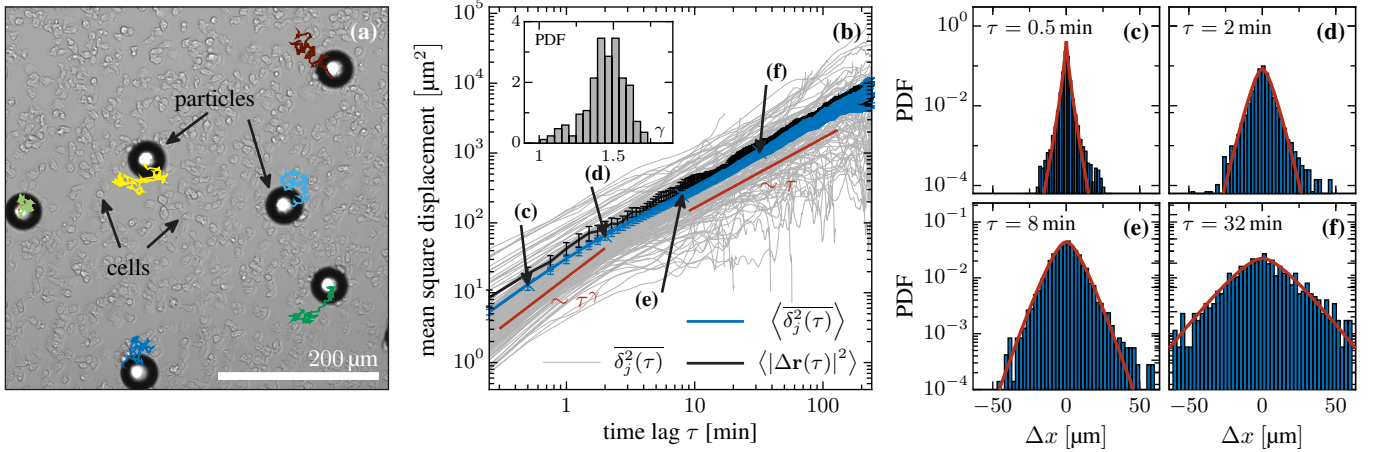


FIG. 1. Characteristics of cargo particle transport on cellular monolayers. **(a)** Illustration of experimental bright-field microscopy recording with particle trajectories displayed as colored overlays (see SM [35] for a movie). Bright spots with a black halo are particle (46 μm diameter). Cells with an extension of about 10 μm appear translucent in the background. **(b)** MSD as function of time: TAMSDs $\overline{\delta_j^2(\tau)}$, Eq. (1), of individual particles (light grey lines), their ensemble average $\langle \overline{\delta_j^2(\tau)} \rangle$ (blue) and the ensemble-averaged MSD $\langle |\Delta \mathbf{r}(\tau)|^2 \rangle$ (black). Error bars indicate 1σ -confidence intervals. These MSDs reveal two distinct regimes: superdiffusion at short time scales and normal diffusion at long times. The inset shows the scaling exponents γ obtained by fitting $\overline{\delta_j^2(\tau)} \sim \tau^\gamma$ to the first three data points of TAMSDs of individual particles (time interval: 45 s). The interaction of a cargo with a single cell may induce anomalous scaling—in line with experimental recordings of individual cell-cargo pairs [25]—whereas the collective long-time particle transport by several cells is normal. Panels **(c)**–**(f)** show the displacement PDFs along the x -axis for different lag times. These PDFs reveal distinctly non-Gaussian statistics, even for long lag times. For short lag times, the displacement PDF is well-fitted by a stretched exponential distribution, proportional to $\exp(-a|\Delta x|^\delta)$, with an exponent $\delta \approx 0.77$ (red line in **(c)**). The red lines in panels **(d)**–**(f)** depict the predicted displacement distributions, based on heterogeneous Brownian motion [cf. Eqs. (5) and main text for details].

MSD crossover from superdiffusive spreading to normal diffusion. Position time traces $\mathbf{r}_j(t)$ of length T of an individual particle j are evaluated in terms of the time-averaged MSD (TAMSD) [40]

$$\overline{\delta_j^2(\tau)} = \frac{1}{T-\tau} \int_0^{T-\tau} [\mathbf{r}_j(t+\tau) - \mathbf{r}_j(t)]^2 dt, \quad (1)$$

where τ is the lag time. The ensemble mean-TAMSD is defined as $\langle \overline{\delta_j^2(\tau)} \rangle = N^{-1} \sum_{j=1}^N \overline{\delta_j^2(\tau)}$. From an ensemble of particles one can also determine the ensemble-averaged MSD $\langle |\Delta \mathbf{r}(\tau)|^2 \rangle = N^{-1} \sum_{j=1}^N [\mathbf{r}_j(\tau) - \mathbf{r}_j(0)]^2$. In an ergodic system the TAMSD converges to the ensemble-averaged MSD in the long time limit $\tau/T \rightarrow 0$; otherwise the dynamics is non-ergodic [40–42].

The results for MSD and TAMSD are displayed in Fig. 1(b). The TAMSDs (light grey lines) reveal a large amplitude spread, indicating significant differences in the transport of individual particles. Their ensemble average, displayed as the blue line, exhibits two regimes: superdiffusion $\langle \Delta \mathbf{r}(\tau)^2 \rangle \simeq \tau^\gamma$ at short lag times with an anomalous diffusion exponent of approximately $\gamma \approx 1.45$ (median) and normal diffusion ($\gamma \approx 1$) at long lag times. Before the crossover time $\tau \approx 2$ min, individual TAMSD scaling exponents vary between $\gamma \approx 1.33$ and 1.57 (1σ -interval); the inset in Fig. 1(b) shows a histogram of the exponents γ obtained from fits to TAMSDs.

A similar superdiffusive scaling was observed for the

MSD of single cell trajectories [43–47] and is reflected in the trajectories of cargo particles transported by an individual cell [25]. The crossover time to normal diffusion corresponds to a length scale that is comparable to the average cell size (5 to 10 μm in radius). We thus conclude that the short-time superdiffusive scaling reflects the action of individual cells, while the long-term normal diffusion corresponds to collective particle transport involving many cells.

Non-Gaussian displacement distributions. The PDFs of the particle displacements $\Delta \mathbf{r}_j(t, \tau) = \mathbf{r}_j(t + \tau) - \mathbf{r}_j(t)$ are shown in Figs. 1(c-f) for different lag times τ . The lag times were chosen from the superdiffusive regime (Fig. 1(c), $\tau = 0.5$ min), close to the crossover time (Fig. 1(d), $\tau = 2$ min), and from the diffusive regime (Figs. 1(e) and (f) with $\tau = 8$ and 32 min), respectively. Notably, all displacement PDFs are non-Gaussian, with a positive excess kurtosis implying a leptokurtic PDF with a more pronounced peak at zero and heavier tails as compared to a Gaussian distribution. At short lag times, the displacement PDF is well approximated by a stretched exponential, proportional to $\exp(-a|\Delta x|^\delta)$ with $\delta \approx 0.77$. With increasing lag time, the PDF changes to a non-Gaussian shape with exponential tails ($\delta \approx 1$) in the Fickian regime ($\gamma = 1$). Below, we describe this exponential PDF by a heterogeneous Brownian diffusion model. We also invoke tempered fractional

Laplace motion as a model for all lag times.

DACF indicates Brownian motion. The ACF of the displacements $\Delta \mathbf{r}_j(\tau)$ of particle j is defined as

$$C_\tau^{(j)}(\Delta) = \overline{\Delta \mathbf{r}_j(t + \Delta, \tau) \cdot \Delta \mathbf{r}_j(t, \tau)} \quad (2)$$

$$= \frac{1}{T - \Delta - \tau} \int_0^{T - \Delta - \tau} \Delta \mathbf{r}_j(t + \Delta, \tau) \cdot \Delta \mathbf{r}_j(t, \tau) dt$$

and measures the degree of correlation between a particle displacement $\Delta \mathbf{r}_j(t, \tau)$ in a time interval τ starting at time t and a displacement in an interval of the same length τ , beginning at the later time $t + \Delta$. For small time shifts Δ , the displacements are highly correlated, whereas the correlations decay to zero at longer Δ . The value of the DACF at $\Delta = 0$ is identical to the TAMSD $\overline{\delta_j^2(\tau)}$, cf. Eq. (1). We focus on the Δ -dependence of the normalized DACF $\tilde{C}_\tau^{(j)}(\Delta) = C_\tau^{(j)}(\Delta)/C_\tau^{(j)}(0)$ as well as on its ensemble mean $\langle \tilde{C}_\tau(\Delta) \rangle = N^{-1} \sum_{j=1}^N \tilde{C}_\tau^{(j)}(\Delta)$. The temporal decay of the ensemble-averaged DACF is shown in Fig. 2(a) for different time lags τ ; the DACFs of individual particle trajectories, together with their ensemble average, are displayed in the inset for $\tau = 2$ min as an example. As expected, the degree of correlation increases with τ . Notably, the correlations decrease linearly as a function of Δ for time lags τ in the diffusive regime and are essentially zero for time shifts $\Delta \geq \tau$. This is a signature of independent steps in normal Brownian motion, for which the renormalized DACF takes the triangular shape $\tilde{C}_\tau(\Delta) = 1 - |\Delta|/\tau$ for $0 \leq |\Delta| \leq \tau$ and 0 otherwise [35]. In Fig. 2(b) we show the DACFs as a function of the rescaled time shift Δ/τ . Indeed, the data collapse onto a single master curve for all time lags $\tau \geq 2$ min, underlining that particle displacements become independent at times of several minutes and beyond.

Fickian yet non-Gaussian particle transport. Our analysis above reveals that polystyrene spheres on a carpet of cells show distinct characteristics of Brownian motion above the crossover time: the MSD increases linearly and the DACF has a triangular shape. However, the displacement PDFs are non-Gaussian for all considered lag times. We tested whether the non-Gaussian statistic arises from non-stationary dynamics of the system but did not detect any statistically significant changes in the bead dynamics over time (see SM [35]).

Non-Gaussian displacement PDFs together with a linear-in-time MSD were observed in different stationary systems, i.a., colloids diffusing along linear tubes or through entangled actin networks [48]. Such observations may arise when the diffusion coefficient of a diffusing particle follows a stochastic diffusion process itself (‘diffusing diffusivity’) [49–53]. If the temporal diffusivity variation is slower than the experimentally relevant time scales, the diffusivity is effectively constant in time but randomly distributed across the diffusing particles [54, 55]. The PDF of diffusivities across the ensemble introduces an additional level of annealed disorder, also called ‘super-

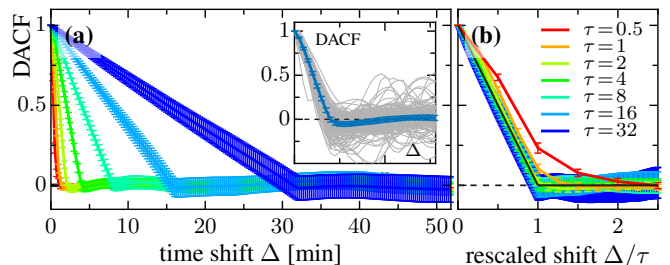


FIG. 2. (a) Ensemble-averaged DACFs for different lag times τ as listed in the right panel (all times in minutes). In the inset, grey lines show single-particle DACFs $\tilde{C}_\tau^{(j)}(\Delta)$ for lag time $\tau = 2$ min. The ensemble average $\langle \tilde{C}_\tau(\Delta) \rangle$ is depicted in blue—error bars indicate 3σ -confidence intervals. Panel (b) shows the same data as in panel (a), as function of the rescaled time shift Δ/τ . For lag times $\tau \geq 2$ min, the DACF collapses onto a triangular correlation function (black solid line), in line with Brownian motion [35].

statistics’ [56]. For ensembles of active particles superstatistical diffusivities and speeds were recently analyzed theoretically [57, 58].

Superstatistics of diffusion coefficients. Long-time particle motion is Fickian, but individual diffusion coefficients D_j of particles j vary across the ensemble, resulting in the amplitude scatter of individual TAMSDs (grey lines) in Fig. 1(b). We expect that this variability is caused by variations in the size and activity within the population of cells (as resolved on the single cell level [47]). Moreover, the cell density varies in space due to finite number fluctuations. The spread in D_j may be enhanced by tug-of-war-style competition between individual cells to which the cargo particle is attached. Even though the statistical properties are identical in the long-time limit (independent increments, normal diffusion), quantitative differences in the diffusivities of individual particles are thus expected.

To test the conjecture that the spread in particle diffusivities may explain the non-Gaussian displacement distributions, we derive the distribution of diffusivities directly from experimental data by estimating the D_j values of individual cargo particles from their TAMSDs via $\hat{D}_j = \overline{\delta_j^2(\tau)}/(4\tau)$. Fig. 3 shows histograms of the D_j estimates for three different lag times τ . All histograms are nicely fitted by a gamma PDF

$$P(D) = \frac{1}{\Gamma(\alpha)D_\beta} \left(\frac{D}{D_\beta}\right)^{\alpha-1} \exp\left(-\frac{D}{D_\beta}\right) \quad (3)$$

with shape parameter α and scale parameter D_β . The goodness of fit can be judged from the cumulative distributions shown in the insets of Fig. 3, where the line corresponds to the fit and the color-shaded region is the 2σ -confidence interval of the empirical distribution. The gamma distributions are consistent over time, i.e., the inferred parameter values are independent of the chosen lag time τ and yield a mean diffusion coefficient of

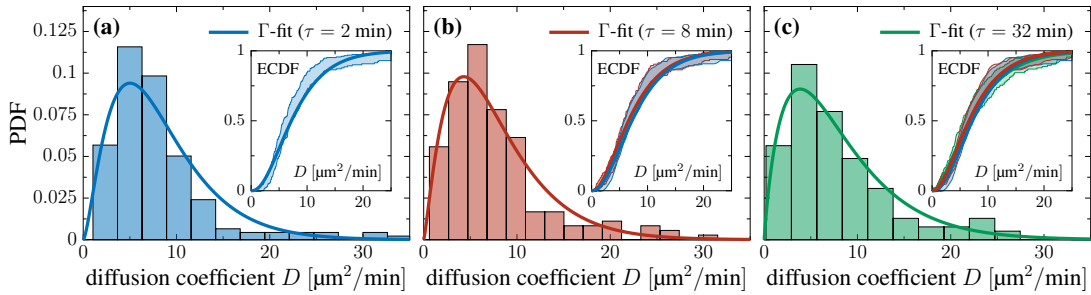


FIG. 3. Histograms of diffusion coefficients for different lag times τ . Solid lines: fits with a gamma distribution [Eq. (3)], inferred by maximum likelihood estimation: (a) $\alpha = 2.55$, $D_\beta = 3.23 \mu\text{m}^2/\text{min}$, (b) $\alpha = 2.26$, $D_\beta = 3.40 \mu\text{m}^2/\text{min}$ and (c) $\alpha = 1.91$, $D_\beta = 4.24 \mu\text{m}^2/\text{min}$. Sample means of diffusion coefficients: (a) $\langle D \rangle = (8.2 \pm 0.5) \mu\text{m}^2/\text{min}$ for $\tau = 2$ min, (b) $\langle D \rangle = (7.7 \pm 0.4) \mu\text{m}^2/\text{min}$ for $\tau = 8$ min, and (c) $\langle D \rangle = (8.0 \pm 0.5) \mu\text{m}^2/\text{min}$ for $\tau = 32$ min. Insets show the corresponding cumulative distributions: lines represent fits and color-shaded regions are 2σ -confidence intervals of the empirical distribution function (ECDF). In the inset of panel (b), the ECDF from panel (a) is shown as an overlay; the inset of panel (c) contains all three ECDFs. There are no statistically significant differences.

$\langle D \rangle \approx 8 \mu\text{m}^2/\text{min}$ in all cases (see caption of Fig. 3 for exact numbers). The consistency of these values supports our conjecture that long-time active transport of microparticles on a carpet of motile cells is governed by heterogeneous Brownian motion.

Prediction of displacement PDFs. We verified the consistency of our superstatistical model by comparison of the empirical displacement PDFs to the model prediction. For normal Brownian diffusion, the displacement PDF (given the diffusion coefficient D) is Gaussian: $\rho(\Delta\mathbf{r}, \tau|D) = (4\pi D\tau)^{-1} \exp[-|\Delta\mathbf{r}|^2/(4D\tau)]$. The displacement PDF of an ensemble of particles with different diffusivities is then obtained by averaging with respect to the distribution of diffusion coefficients $P(D)$ [54, 56]:

$$\langle \rho(\Delta\mathbf{r}, \tau) \rangle = \int_0^\infty \rho(\Delta\mathbf{r}, \tau|D) P(D) dD. \quad (4)$$

The corresponding displacement PDFs of the x - and y -components of $\Delta\mathbf{r}$ are obtained by marginalization. In the diffusive regime, they were found to be statistically independent (linear correlation coefficient below 0.02 in all cases). We focus on displacements along the x -axis [59]. Using the gamma distribution model $P(D)$ to describe the heterogeneity in the diffusion coefficients and the Gaussian propagator $\rho(\Delta\mathbf{r}, \tau|D)$, we obtain the displacement PDF

$$\langle \rho(\Delta x, \tau) \rangle = \mathcal{N} \frac{|\Delta x|^{\alpha-1/2}}{(D_\beta\tau)^{\alpha/2+1/4}} K_{\alpha-1/2} \left(\frac{|\Delta x|}{(D_\beta\tau)^{1/2}} \right) \quad (5a)$$

$$\simeq \frac{1}{2^\alpha \Gamma(\alpha)} \frac{|\Delta x|^{\alpha-1}}{(D_\beta\tau)^{\alpha/2}} \exp \left[-\frac{|\Delta x|}{(D_\beta\tau)^{1/2}} \right], \quad (5b)$$

where $\mathcal{N} = 2^{1/2-\alpha}/[\sqrt{\pi}\Gamma(\alpha)]$ is a normalization constant and $K_\nu(x)$ denotes the modified Bessel function of the second kind. Asymptotically, an exponential tail emerges with a power-law correction in $|\Delta x|$ [Eq. (5b)] that vanishes in the case of exponentially distributed diffusion coefficients ($\alpha = 1$) [35]. By derivation, the

displacement PDF depends on the similarity variable $|\Delta x|/\sqrt{\tau}$ only, reflecting the normal diffusive behavior $\Delta x^2 \sim \tau$. The PDF (5a) is compared to experimental data in Fig. 1(d-f). Note that this is not a fit since all parameters in Eqs. (5) were derived from the empirical PDF of diffusion coefficients (Fig. 3). The agreement of the displacement PDFs confirms our hypothesis that individual cargo particles perform Brownian motion with randomly distributed diffusivities.

Discussion. We found that the nonequilibrium transport of microparticles in an active bath of cells displays a crossover from superdiffusion to Fickian transport with pronounced non-Gaussian displacement PDFs. While the dynamics of each particle becomes Brownian, the diffusivity varies across the ensemble [54]. This variation may arise from tug-of-war between multiple cells simultaneously attached to the cargo particle. The tug-of-war may lead to repeated unsuccessful attempts to move the cargo in a given time window. Intermittent motion with distributed immobilization events can be described by subordination of a parent process with a waiting time PDF [60, 61]. If the subordinator is a gamma distribution, Brownian motion stays Fickian yet the displacements follow a Laplace PDF [62, 63]. If the parent process is fractional Brownian motion, a Gaussian process with power-law correlated increments [64, 65], the subordination by the gamma distribution produces a PDF with stretched tails proportional to $\exp(-a|\Delta x|^\delta)$, the stretching exponent of which is $\delta = 2/(1 + \gamma)$ [66]. The DACF derived from our experimental data at short times indeed shows positive values beyond the rescaled time shift $\Delta/\tau = 1$, reminiscent of fractional Brownian motion. Thus, assuming fractional Laplace motion (FLM) for the cargo particle transport dynamics, superdiffusion in the short-time regime with an exponent of $\gamma \approx 1.45$ (median of the observed exponents, cf. Fig. 1) would imply a stretching exponent of $\delta \approx 0.82$, which is close to the experimentally inferred $\delta \approx 0.77$ as shown in Fig. 1(c).

Assuming that the power-law correlations have a finite cutoff that reflects the observed crossover from super- to Fickian diffusion, the motion at long times would change from $\langle \Delta \mathbf{r}(\tau)^2 \rangle \simeq t^\gamma$ to $\simeq t$ [67], and the displacement PDF exhibits exponential tails ($\delta = 1$), in line with our experimental observations. More refined data will be needed to connect the observed motion with potential tug-of-war immobilization events. Furthermore, it will be of interest to discuss asymptotic Laplace displacement PDFs and FLM in a wider context of anomalous diffusion processes in the future [51, 61, 68, 69].

Non-Gaussian statistics due to (dynamic) heterogeneity has already been reported for acetylcholine receptors on live muscle cell membranes [70] and for cytoplasmic mRNA molecules in both *E. coli* and yeast [71]. Here, we demonstrate that anomalous effects may also arise at the level of interacting cells when collectively moving passive microobjects. Since cell-cell heterogeneity and fluctuation-dominated dynamics are ubiquitous in biological systems, our findings are relevant beyond our specific model system, for instance, when microparticles are exposed to migrating neutrophils. Generally, foreign bodies that interact with a dynamic tissue environment are key to many medical applications—oral vaccination strategies [72] or the assimilation of environmental microplastics in the body [73] both rely on the intestinal uptake of microparticles. Options to guide the cell-driven microtransport by chemical gradients [38] make this process particularly attractive for drug delivery applications.

This research has been partially funded by Deutsche Forschungsgemeinschaft (DFG), grant 318763901–SFB1294 (R.G., L.B., T.M., and C.B.), 116203121 – BE 3978/3-3 (S.S.P. and C.B.), and ME 1535/12-1 (R.M.). We thank Maike Stange for valuable comments on the manuscript and support regarding the experiment, as well as Kirsten Sachse for supporting lab routines.

* Correspondence should be addressed to: rgrossmann@uni-potsdam.de, rmetzler@uni-potsdam.de, beta@uni-potsdam.de

- [1] P. Romanczuk, M. Bär, W. Ebeling, B. Lindner, and L. Schimansky-Geier, Active Brownian particles, *Eur. Phys. J.: Spec. Top.* **202**, 1 (2012).
- [2] C. Bechinger, R. Di Leonardo, H. Löwen, C. Reichhardt, G. Volpe, and G. Volpe, Active particles in complex and crowded environments, *Rev. Mod. Phys.* **88**, 045006 (2016).
- [3] R. Soto and R. Golestanian, Self-assembly of catalytically active colloidal molecules: Tailoring activity through surface chemistry, *Phys. Rev. Lett.* **112**, 068301 (2014).
- [4] D. Feldmann, S. R. Maduar, M. Santer, N. Lomadze, O. I. Vinogradova, and S. Santer, Manipulation of small particles at solid liquid interface: light driven diffusio-osmosis, *Sci. Rep.* **6**, 36443 (2016).
- [5] D. Feldmann, P. Arya, N. Lomadze, A. Kopyshev, and S. Santer, Light-driven motion of self-propelled porous Janus particles, *Appl. Phys. Lett.* **115**, 263701 (2019).
- [6] X. Zheng, B. ten Hagen, A. Kaiser, M. Wu, H. Cui, Z. Silber-Li, and H. Löwen, Non-Gaussian statistics for the motion of self-propelled Janus particles: Experiment versus theory, *Phys. Rev. E* **88**, 032304 (2013).
- [7] H. C. Berg, *Random walks in biology* (Princeton University Press, 1993).
- [8] H. C. Berg, *E. coli in Motion* (Springer, 2004).
- [9] A. Be'er and G. Ariel, A statistical physics view of swarming bacteria, *Mov. Ecol.* **7**, 9 (2019).
- [10] I. S. Aranson, ed., *Physical models of cell motility* (Springer, 2016).
- [11] A. Altshuler, O. Lauber Bonomo, N. Gorohovsky, S. Marchini, E. Rosen, O. Tal-Friedman, S. Reuveni, and Y. Roichman, Environmental memory facilitates search with home returns [arXiv:2306.12126](https://arxiv.org/abs/2306.12126) (2023).
- [12] O. Dauchot and V. Démery, Dynamics of a self-propelled particle in a harmonic trap, *Phys. Rev. Lett.* **122**, 068002 (2019).
- [13] D. Horvath, C. Slabý, Z. Tomori, A. Hovan, P. Miskovsky, and G. Bánó, Bouncing dynamics of inertial self-propelled particles reveals directional asymmetry, *Phys. Rev. E* **107**, 024603 (2023).
- [14] G. M. Viswanathan, M. G. Da Luz, E. P. Raposo, and H. E. Stanley, *The physics of foraging: an introduction to random searches and biological encounters* (Cambridge University Press, 2011).
- [15] M. Marchetti, J. Joanny, S. Ramaswamy, T. Liverpool, J. Prost, M. Rao, and R. Simha, Hydrodynamics of soft active matter, *Rev. Mod. Phys.* **85**, 1143 (2013).
- [16] S. Shankar, A. Souslov, M. J. Bowick, M. C. Marchetti, and V. Vitelli, Topological active matter, *Nat. Rev. Phys.* **4**, 380 (2022).
- [17] M. E. Cates and J. Tailleur, Motility-induced phase separation, *Annu. Rev. Condens. Matter Phys.* **6**, 219 (2015).
- [18] H. Chaté, Dry aligning dilute active matter, *Annu. Rev. Condens. Matter Phys.* **11**, 189 (2020).
- [19] M. Bär, R. Großmann, S. Heidenreich, and F. Peruni, Self-propelled rods: Insights and perspectives for active matter, *Annu. Rev. Condens. Matter Phys.* **11**, 441 (2020).
- [20] A. P. Solon, Y. Fily, A. Baskaran, M. E. Cates, Y. Kafri, M. Kardar, and J. Tailleur, Pressure is not a state function for generic active fluids, *Nat. Phys.* **11**, 673 (2015).
- [21] F. Ginot, I. Theurkauff, D. Levis, C. Ybert, L. Bocquet, L. Berthier, and C. Cottin-Bizonne, Nonequilibrium equation of state in suspensions of active colloids, *Phys. Rev. X* **5**, 011004 (2015).
- [22] N. Nikola, A. P. Solon, Y. Kafri, M. Kardar, J. Tailleur, and R. Voituriez, Active particles with soft and curved walls: Equation of state, ratchets, and instabilities, *Phys. Rev. Lett.* **117**, 098001 (2016).
- [23] O. Hallatschek, S. S. Datta, K. Drescher, J. Dunkel, J. Elgeti, B. Waclaw, and N. S. Wingreen, Proliferating active matter, *Nat. Rev. Phys.* **5**, 407–419 (2023).
- [24] M. J. Bowick, N. Fakhri, M. C. Marchetti, and S. Ramaswamy, Symmetry, thermodynamics, and topology in active matter, *Phys. Rev. X* **12**, 010501 (2022).
- [25] V. Lepro, R. Großmann, S. Sharifi Panah, O. Nagel, S. Klumpp, R. Lipowsky, and C. Beta, Optimal cargo size for active diffusion of biohybrid microcarriers, *Phys. Rev. Appl.* **18**, 034014 (2022).
- [26] G. Lambert, D. Liao, and R. H. Austin, Collective escape

- of chemotactic swimmers through microscopic ratchets, *Phys. Rev. Lett.* **104**, 168102 (2010).
- [27] H. Xu, M. R. Nejad, J. M. Yeomans, and Y. Wu, Geometrical control of interface patterning underlies active matter invasion, *Proc. Natl. Acad. Sci. USA* **120**, e2219708120 (2023).
- [28] A. Sokolov, M. M. Apodaca, B. A. Grzybowski, and I. S. Aranson, Swimming bacteria power microscopic gears, *Proc. Natl. Acad. Sci. USA* **107**, 969 (2009).
- [29] S. Ray, J. Zhang, and Z. Dogic, Rectified rotational dynamics of mobile inclusions in two-dimensional active nematics, *Phys. Rev. Lett.* **130**, 238301 (2023).
- [30] S. A. Mallory, C. Valeriani, and A. Cacciuto, Curvature-induced activation of a passive tracer in an active bath, *Phys. Rev. E* **90**, 032309 (2014).
- [31] X.-L. Wu and A. Libchaber, Particle diffusion in a quasi-two-dimensional bacterial bath, *Phys. Rev. Lett.* **84**, 3017 (2000).
- [32] G. L. Miño, J. Dunstan, A. Rousselet, E. Clément, and R. Soto, Induced diffusion of tracers in a bacterial suspension: theory and experiments, *J. Fluid. Mech.* **729**, 423–444 (2014).
- [33] K. C. Leptos, J. S. Guasto, J. P. Gollub, A. I. Pesci, and R. E. Goldstein, Dynamics of enhanced tracer diffusion in suspensions of swimming eukaryotic microorganisms, *Phys. Rev. Lett.* **103**, 198103 (2009).
- [34] F. Guzmán-Lastra, H. Löwen, and A. J. Mathijssen, Active carpets drive non-equilibrium diffusion and enhanced molecular fluxes, *Nat. Commun.* **12**, 1906 (2021).
- [35] See Supplemental Material for complementary technical information.
- [36] S. J. Annesley and P. R. Fisher, *Dictyostelium discoideum*—a model for many reasons, *Mol. Chem. Biochem.* **329**, 73 (2009).
- [37] W. F. Loomis, D. Fuller, E. Gutierrez, A. Groisman, and W.-J. Rappel, Innate non-specific cell substratum adhesion, *PLoS one* **7**, e42033 (2012).
- [38] O. Nagel, M. Frey, M. Gerhardt, and C. Beta, Harnessing motile amoeboid cells as trucks for microtransport and -assembly, *Adv. Sci.* **6**, 1801242 (2018).
- [39] S. S. Panah, R. Großmann, V. Lepro, and C. Beta, Cargo size limits and forces of cell-driven microtransport, *arXiv:2305.15298* (2023).
- [40] E. Barkai, Y. Garini, and R. Metzler, Strange kinetics of single molecules in living cells, *Phys. Today* **65**, 29 (2012).
- [41] Y. He, S. Burov, R. Metzler, and E. Barkai, Random time-scale invariant diffusion and transport coefficients, *Phys. Rev. Lett.* **101**, 058101 (2008).
- [42] S. Burov, R. Metzler, and E. Barkai, Aging and nonergodicity beyond the Khinchin theorem, *Proc. Natl. Acad. Sci. USA* **107**, 13228 (2010).
- [43] P. Dieterich, R. Klages, R. Preuss, and A. Schwab, Anomalous dynamics of cell migration, *Proc. Natl. Acad. Sci. USA* **105**, 459 (2008).
- [44] L. Li, S. F. Nørrelykke, and E. C. Cox, Persistent cell motion in the absence of external signals: A search strategy for eukaryotic cells, *PLoS one* **3**, e2093 (2008).
- [45] H. Takagi, M. J. Sato, T. Yanagida, and M. Ueda, Functional analysis of spontaneous cell movement under different physiological conditions, *PLoS one* **3**, e2648 (2008).
- [46] N. Makarava, S. Menz, M. Theves, W. Huisinga, C. Beta, and M. Holschneider, Quantifying the degree of persistence in random amoeboid motion based on the Hurst exponent of fractional Brownian motion, *Phys. Rev. E* **90**, 042703 (2014).
- [47] A. G. Cherstvy, O. Nagel, C. Beta, and R. Metzler, Non-Gaussianity, population heterogeneity, and transient superdiffusion in the spreading dynamics of amoeboid cells, *Phys. Chem. Chem. Phys.* **20**, 23034 (2018).
- [48] B. Wang, S. M. Anthony, S. C. Bae, and S. Granick, Anomalous yet Brownian, *Proc. Natl. Acad. Sci. USA* **106**, 15160 (2009).
- [49] M. V. Chubynsky and G. W. Slater, Diffusing diffusivity: A model for anomalous, yet Brownian, diffusion, *Phys. Rev. Lett.* **113**, 098302 (2014).
- [50] Y. Lanoiselée, N. Moutal, and D. S. Grebenkov, Diffusion-limited reactions in dynamic heterogeneous media, *Nat. Commun.* **9**, 4398 (2018).
- [51] A. Sabri, X. Xu, D. Krapf, and M. Weiss, Elucidating the origin of heterogeneous anomalous diffusion in the cytoplasm of mammalian cells, *Phys. Rev. Lett.* **125**, 058101 (2020).
- [52] E. Yamamoto, T. Akimoto, A. Mitsutake, and R. Metzler, Universal relation between instantaneous diffusivity and radius of gyration of proteins in aqueous solution, *Phys. Rev. Lett.* **126**, 128101 (2021).
- [53] K. Sakamoto, T. Akimoto, M. Muramatsu, M. S. P. Sansom, R. Metzler, and E. Yamamoto, Heterogeneous biological membranes regulate protein partitioning via fluctuating diffusivity, *PNAS Nexus* **2**, pgad258 (2023).
- [54] A. V. Chechkin, F. Seno, R. Metzler, and I. M. Sokolov, Brownian yet non-Gaussian diffusion: From superstatistics to subordination of diffusing diffusivities, *Phys. Rev. X* **7**, 021002 (2017).
- [55] V. Sposini, A. V. Chechkin, F. Seno, G. Pagnini, and R. Metzler, Random diffusivity from stochastic equations: comparison of two models for Brownian yet non-Gaussian diffusion, *New J. Phys.* **20**, 043044 (2018).
- [56] C. Beck and E. G. Cohen, Superstatistics, *Physica A* **322**, 267 (2003).
- [57] E. Lemaitre, I. M. Sokolov, R. Metzler, and A. V. Chechkin, Non-Gaussian displacement distributions in models of heterogeneous active particle dynamics, *New J. Phys.* **25**, 013010 (2023).
- [58] S. M. J. Khadem, N. H. Siboni, and S. H. L. Klapp, Transport and phase separation of active Brownian particles in fluctuating environments, *Phys. Rev. E* **104**, 064615 (2021).
- [59] Analogous results are obtained for displacements along the y -axis.
- [60] M. Magdziarz, A. Weron, K. Burnecki, and J. Klafter, Fractional Brownian motion versus the continuous-time random walk: A simple test for subdiffusive dynamics, *Phys. Rev. Lett.* **103**, 180602 (2009).
- [61] Z. R. Fox, E. Barkai, and D. Krapf, Aging power spectrum of membrane protein transport and other subordinated random walks, *Nat. Commun.* **12**, 6162 (2021).
- [62] D. B. Madan and E. Seneta, The variance gamma (v.g.) model for share market returns, *J. Bus.* **63**, 511 (1990).
- [63] D. B. Madan, P. P. Carr, and E. C. Chang, The variance gamma process and option pricing, *Rev. Financ.* **2**, 79 (1998).
- [64] B. B. Mandelbrot and J. W. Van Ness, Fractional Brownian motions, fractional noises and applications, *SIAM Rev.* **10**, 422 (1968).
- [65] S. M. J. Khadem, R. Klages, and S. H. L. Klapp, Stochastic thermodynamics of fractional brownian motion, *Phys.*

- [Rev. Res. 4, 043186 \(2022\)](#).
- [66] T. J. Kozubowski, M. M. Meerschaert, and K. Podgórski, Fractional Laplace motion, [Adv. Appl. Probab. 38, 451 \(2006\)](#).
- [67] D. Molina-Garcia, T. Sandev, H. Safdari, G. Pagnini, A. Chechkin, and R. Metzler, Crossover from anomalous to normal diffusion: truncated power-law noise correlations and applications to dynamics in lipid bilayers, [New J. Phys. 20, 103027 \(2018\)](#).
- [68] G. Muñoz-Gil, G. Volpe, M. A. Garcia-March, E. Aghion, A. Argun, C. B. Hong, T. Bland, S. Bo, J. A. Conejero, N. Firbas, *et al.*, Objective comparison of methods to decode anomalous diffusion, [Nat. Commun. 12, 6253 \(2021\)](#).
- [69] H. Seckler and R. Metzler, Bayesian deep learning for error estimation in the analysis of anomalous diffusion, [Nature Commun. 13, 6717 \(2022\)](#).
- [70] W. He, H. Song, Y. Su, L. Geng, B. J. Ackerson, H. Peng, and P. Tong, Dynamic heterogeneity and non-Gaussian statistics for acetylcholine receptors on live cell membrane, [Nat. Commun. 7, 11701 \(2016\)](#).
- [71] T. J. Lampo, S. Stylianidou, M. P. Backlund, P. A. Wiggins, and A. J. Spakowitz, Cytoplasmic RNA-protein particles exhibit non-Gaussian subdiffusive behavior, [Biophys. J. 112, 532 \(2017\)](#).
- [72] E. F. P. Soares and O. M. F. Borges, Oral vaccination through Peyer's patches: Update on particle uptake, [Curr. Drug Deliv. 15, 321 \(2018\)](#).
- [73] E. Pulvirenti, M. Ferrante, N. Barbera, C. Favara, E. Aquilia, M. Palella, A. Cristaldi, G. O. Conti, and M. Fiore, Effects of nano and microplastics on the inflammatory process: In vitro and in vivo studies systematic review, [Front. Biosci. 27, 287 \(2022\)](#).